Evaluation of Low Frequency Electrical and Magnetic Fields in a Electrical Transmission Substation

ROMINA BELTRÁN, EMILY CHAMORRO, CARLOS QUINATOA, JIMMY TOAZA
Department of Electrical Engineering,
University Technical of Cotopaxi,
Av. Simón Rodríguez s/n Barrio El Ejido Sector San Felipe,
Latacunga,
ECUADOR

Abstract: - In recent years, there has been a stagnation in the investigation of the issues related to exposure to electromagnetic fields, as it has been deemed that their presence is not significantly apparent; however, they may induce alterations within the human body and pose certain occupational risks. It is widely accepted that these fields do not emit sufficient energy to effectuate such changes at the atomic level, yet they can have detrimental effects on the health of employees. This article delineates the findings from the assessment of non-ionizing radiation within the premises of the MULALO Electric Transmission Substation, where the reference values for exposure around the generation plant are based on public safety; conversely, within the substation, the relevant values should pertain specifically to workers exposed in occupational settings. Ultimately, these results facilitate an analysis to ascertain whether the emissions from AM No. 155, MAE, TULSMA CEM standards comply with the limits established by the International Commission on Non-Ionizing Radiation Protection, in addition to identifying the most significant values of electric and magnetic fields present within the easement strip.

Key-Words: - Problems, Workers, Radiation, Electromagnetic, Electric.

Received: April 9, 2024. Revised: August 11, 2024. Accepted: October 7, 2023. Published: November 14, 2024.

1 Introduction

The assessment of low-frequency electric and magnetic fields in electrical substations is fundamental to worker health and welfare standards, [1]. This assessment focuses on magnetic fields generated by equipment such as transformers, busbars and cables in secondary substations. To competently conduct the analysis, a methodological approach is used to accurately measure magnetic fields and assess the associated risks, [2]. The methodology outlines protocols for measuring exposure levels and ensures that potential hazards are thoroughly identified and quantified, [2]. This comprehensive process is critical to understanding the potential hazards to which personnel are exposed at medium and low voltage switchgear installations. In addition, the presence of extremely low frequency (ELF) electric fields, especially in the vicinity of high-voltage transmission lines, has prompted the study of their biological effects, raising concerns about environmental impact and workplace safety, [2] . In summary, the integration of these principles provides a sound basis for assessing and mitigating the risks associated with low-frequency electric and magnetic fields in substations, [3]. Studies show that electromagnetic fields (CEM) generated by substations and transformers vary considerably, and many measurements are often below internationally established safety standards. For example, in Aguata, Nigeria, a maximum electric field of 0.7783 V/m was measured, while the magnetic field strength was 1.3317 A/m, which meets International Commission on Non-Ionizing Radiation Protection (ICNIRP) guidelines, [4]. Similarly, measurements near high-voltage power lines in Iran showed average magnetic flux densities below the recommended limits, [5]. However, concerns remain about potential health effects, as several studies have shown that people exposed to ELF magnetic fields exhibit health problems, [6]. This highlights the need for continuous monitoring and thorough risk assessment to ensure safety in these environments. Electric and magnetic fields are quantified using CEM meters and the results are evaluated below with respect to ICNIRP standards. At Aguata, a maximum power density of 1.0365 W/m² was measured, which means that exposure levels are site-specific, [4]. Employees working near transformers have reported symptoms such as fatigue and dizziness, raising great concern about the consequences of prolonged exposure, [6]. A research study conducted in Tehran indicated a possible link between exposure to electromagnetic fields and mental health problems, [7].

Although several studies have identified generally low levels of electromagnetic fields, potential health risks, especially in occupational settings, require thorough assessment and strict compliance with safety standards, [8]. CEM are ubiquitous in modern

society and are a growing problem in the workplace and the environment. These fields can have biological effects, especially in the case of ELF generated by high-voltage power lines or electrical appliances, [9], [10], [11]. A study by [12], evaluated CEM levels in electrical substations and showed that occupationally exposed workers were likely to exceed recommended exposure limits, [13]. Researchers have also studied the biological effects of ELF-CEM exposure and have found evidence of changes in the central and peripheral nervous systems, [14], [15], [16]. The results underline the need for further research on the possible harmful effects of these fields on human health. Regarding regulatory standards, the authors highlight in their contribution the importance of following the protocols established by the ICNIRP to ensure safety, [17]. These recommendations set exposure limits based on available scientific evidence and current research, which suggests that exposure to CEM from substations may pose a risk to human health, [17], [18]. Further research is needed in this area to improve our understanding of exposure to these fields and to develop effective protective measures, [18]. CEM are a combination of electric and magnetic waves that travel simultaneously at the speed of light. The higher the frequency, the more energy the wave transmits; these magnetic fields are created by the accumulation of charge in certain regions of the atmosphere due to the effects of storms, [17], [19].

This section deals with the evaluation of low frequency CEM in a substation. The significance of this evaluation, regarding the safeguarding of human health and the environment, will be articulated, taking into account the potential effects associated with exposure to CEM. Furthermore, the parameters of the study will, specifying the elements that will be examined in the methodology. In addition, the article is structured as follows: the second section deals with the measurement methodology, mathematical methodology, measurement procedures, the applicable legal framework and instrumentation. The third section discusses the treatment of both the measured results and their simulation in order to apply the mathematical methodology. The fourth section presents the simulation of the data using the Least Squares Methods (MLS) method. The fifth section presents additional information, based on observations and location of the measured points in a sketch. Finally, the last sections present conclusions and recommendations, derived from the study carried out.

2 Data Measurement Methodology

The methodology used for measuring non-ionizing radiation from electromagnetic fields followed the regulations established in the internal procedure detailed in [20], [21]. In the case of measurements in substations, the limits to be used are the following: for measurements in the periphery of the substation, the reference values are those of population exposure; inside the substation, the reference values should be those of exposure to occupationally exposed workers. Select the measurement points where there is greater exposure of the worker as a reference point to perform the measurement. Figure 1 shows the procedure to be followed for electric and magnetic field measurements, based mainly on the identification and recognition of the site, determining the different sources of energy to select measurement points where workers are most exposed, carrying out the measurements with equipment that complies with the established regulations.

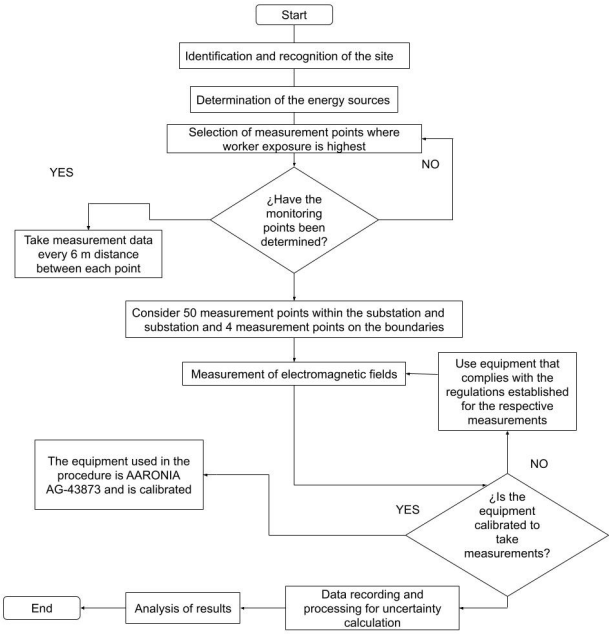

Fig. 1: Internal procedure PE/IPGM/11 measurement of non-ionizing radiations

2.1 Electrical Substations Measurement Procedure

In the case of measurements in substations, the limits to be used are as follows: for measurements in the periphery of the substation, the reference values are those of population exposure; inside the substation, the reference values should be those of exposure to occupationally exposed workers. Select the measurement points where there is the greatest exposure of the worker as a reference point for measurement.

Reference standards for exposure to CEM originating from 60 Hz sources, applicable to both the public and individuals in occupational settings.

In this case measurements in substations the limits to be used are the following: for measurements in the periphery of the substation the reference values are those of population exposure; inside the substation the reference values should be those of exposure to occupationally exposed workers. Select at least two axes that are perpendicular to each other and that cover the entire substation. The location of these axes should have a horizontal separation of 0.2m in addition to the safety distance. The first of the axes should be located in front of the entrance gantry or gantries inside the substation and the center phase of each entrance line gantry should be taken as a reference or first measurement point, then two points should be measured both to the right and to the left with respect to the reference point with an equally spaced separation covering the entrance gantry.

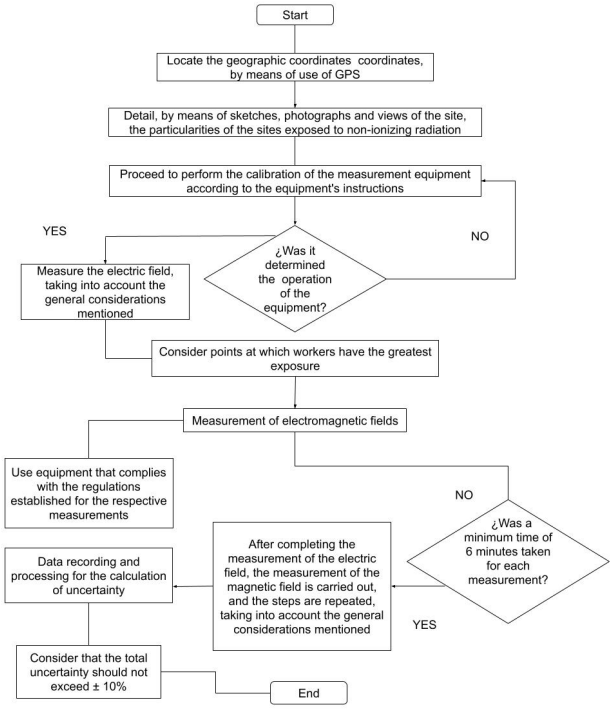

Fig. 2: Procedure for measuring magnetic and electric fields

Figure 2 shows the correct procedure to perform the respective measurements by locating the geographic coordinates, through the use of GPS, the measurement points that have already been defined in the sampling strategy, detailing through sketches, photographs, and views of the site, the particularities of the sites exposed to non-ionizing radiation, proceed to turn on the equipment and set the units and measurement time according to the equipment manual, perform the calibration of the measuring equipment according to the equipment instructions and measure the electric field. Measurement uncertainties arising from calibration, temperature, interference, observed proximity, and parameters and presented as the comprehensive estimated uncertainty of the measurements, ensuring that the total uncertainty does not surpass ± 10%.

2.2 Mathematical Methodology

The moving least squares method was applied, which is a technique used in data analysis and computer graphics to make smooth approximations and fit surfaces from a discrete data set.

2.2.1 MLS Representation

The interpolation method applied was the "griddata" method incorporated in MATLAB, which generates a uniform grid every 5 m that adapts to the original data and fills the information by means of an interpolation based on "biharmonic spline" adjustment. With the fitted meshes the surfaces and contour lines for the electric and magnetic field can be generated. The fitted meshes correspond to the matrices **E** and **B**, which correspond to the input data of the whole analysis process. Once the adjustment meshes and the E and B matrices are available, the MLS adjustment method can be applied.

$$\hat{F} = \Phi \cdot F \tag{1}$$

Where:

- F : It is the original data matrix.
- Φ : It is the fit shape matrix.
- $\hat{F}$: It is the resulting matrix of adjusted values.

The main objective is to obtain the fitting shape matrix Φ, which is given by the equation:

$$\Phi = P' \cdot A^{-1} \cdot B \tag{2}$$

Where:

- P : It is the vector of polynomials chosen, P' is the transpose of P .
- A^{-1} :Pitch matrix.
- B : Pitch matrix.

The polynomial matrix is made up of polynomials of a given degree. The higher the degree of the polynomial, the smoother the surface will be. In this case it was determined that the results would be sufficiently satisfactory with second order.

$$P = \begin{bmatrix} p_{11} & p_{1n} \\ p_{n1} & p_{nn} \end{bmatrix} \tag{3}$$

Where each p_{ij} value is obtained by evaluating the following expression:

$$p_{ij} = 1 + x_{ij} + y_{ij} + x_{ij}^2 + x_{ij} \cdot y_{ij} + y_{ij}^2 \quad (4)$$

Once the polynomial matrix is assembled, we proceed with the other parameters. The step matrices **A** and **B** are matrices that are calculated as a function of the polynomial matrix and the diagonal matrix of weights ***W***. They are calculated solely for the purpose of saving computation time and organizing mathematical formulas. The expressions for calculating the step matrices are given by:

$$A = P' \cdot W \cdot P \quad (5)$$

$$B = P' \cdot W \quad (6)$$

Where matrix **W**, as mentioned above, is the weight matrix. This matrix is a diagonal matrix, where each matrix entry is a variable determined by the weight function ω. The matrix **W**, will have the following form:

$$W = \begin{bmatrix} \omega_1 & 0 \\ 0 & \omega_n \end{bmatrix} \quad (7)$$

To calculate the value of each weight ω_k the following expression is applied:

$$\omega_k \begin{cases} \frac{2}{3} - 4r_k^2 + 4r_k^3 & si \quad r_k \leq \frac{1}{2} \\ \frac{4}{3}4r_k + 4r_k^2 - \frac{4}{3}r_k^3 & si \quad \frac{1}{2} < r_k \leq 1 \\ 0 & si \quad r < 1 \end{cases} \quad (8)$$

The value of β is a constant, and depending on the configuration of the problem and the criteria of the data analyst, it can range from:

$$2.0 \leq \beta \leq 5.0 \quad (9)$$

For this case study it was established that β = 3.0. On the other hand, the value of the parameter r_k is calculated by the following equation:

$$r_k \frac{\|F_k - F_k + 1\|}{d_{mi}} \quad (10)$$

In other words, the magnitude between a point and its adjacency is considered, and divided for the parameter d_{mi}. The parameter d_{mi} is known as the radius of convergence, and is one of the most important parameters in the MLS process, since it determines how smooth the resulting surface will be. For this particular case study, a convergence radius of **5** was established, since it coincides with the initial meshing every 5 m. A convergence radius smaller than 5 may have no effect on the result, while a convergence radius larger than 5 may exaggeratedly smooth the surface, [22]. The following flowchart MLS shows the process followed to obtain the CEM (Figure 3).

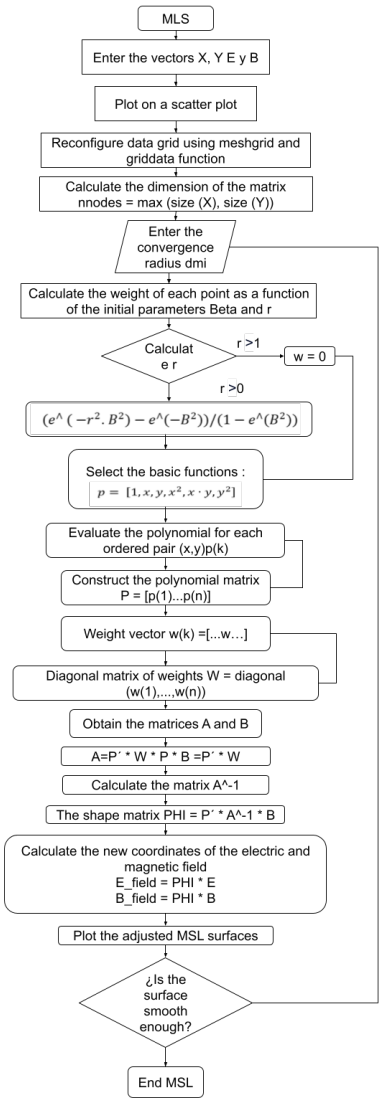

Fig. 3: Procedure for obtaining MLS data matrices

3 Results Processing

3.1 Measurement Results

In the results of the measurement of electric and magnetic fields 54 points were considered, the first 50 points are points of analysis within the substation and the remaining 4 are points of analysis of the boundaries of the S/E, it is considered that the greatest presence of electric fields are at points P5, P6,P8,P9,P17,P19,P20,P48 and of the boundaries is point P2, while in the magnetic field the greatest

presence is identified in points P25,P26,P27,P28 and in the points of the boundaries point P4 is considered with the greatest presence, these data are shown in Table 1.

Table 1. Measurement results

Measuring point	X	Y	Electric field V/m	Magnetic field uT
Measurement points within the S/E				
P5	766282	9911973	1000	0.713
P6	766282	9911962	948.9	0.735
P7	766282	9911952	935.9	0.9236
P8	766282	9911944	1001.4	0.786
P9	766282	9911935	995	0.7019
P17	766259	9912000	107.5	1.14
P19	766229	9912013	1868	1.223
P20	766231	9912004	1477	1.154
P48	766185	9911951	1176.5	1.277
P25	766232	9911966	1656	2.064
P26	766231	9911959	3524	2.952
P27	766231	9911952	3024	2.712
P28	766231	9911945	763.8	2.294
Measurement points within the S/E				
P2	766298	9911980	110.5	1.275
P4	766146	9911980	240.9	1.352

3.2 Final Results

Table 2. Final results

Measuring point	Electric field V/m	Uncertainty ±U(V/m)	Magnetic field uT	Uncertain ±U(uT)	Reference level
P5	1000	8.42	0.713	0.21	8333V/m ;417uT
P6	948.9	8	0.735	0.21	8333V/m ;417uT
P7	935.9	7.89	0.9236	0.21	8333V/m ;417uT
P8	1001.4	8.43	0.786	0.21	8333V/m ;417uT
P9	995	8.38	0.7019	0.21	8333V/m ;417uT
P17	107.5	1.13	1.14	0.21	8333V/m ;417uT
P18	432.1	3.77	0.76	0.21	8333V/m ;417uT
P19	1868	15.54	1.223	0.21	8333V/m ;417uT
P20	1477	12.33	1.154	0.21	8333V/m ;417uT
P48	1176.5	9.87	1.277	0.21	8333V/m ;417uT
P25	1656	13.8	2.064	0.21	8333V/m ;417uT
P26	3524	29.12	2.952	0.21	8333V/m ;417uT
P27	3024	25.02	2.712	0.21	8333V/m ;417uT
P28	763.8	6.49	2.294	0.21	8333V/m ;417uT
Measuring points on the boundaries					
P2	110.5	1.15	1.275	0.21	4167vV/m ;83uT
P4	240.9	2.21	1.352	0.21	4167vV/m ;83uT

With the measurement points that have a higher presence of electromagnetic fields, the corresponding verification is performed with the declared uncertainty based on the expanded uncertainty multiplied by a coverage factor k=2, which guarantees an approximate confidence level of 95%. Therefore the values of Table 2, of the final results are governed by the TULSMA regulations.

3.3 Operation data

Table 3, Table 4 identifies the mean which is the measure of central tendency that provides an overall representation of the data set, the mode is the value useful for identifying the most common value in a data set.

The standard deviation is a measure of dispersion that indicates how much the individual values deviate from the mean in a data set, quartile 1is the value that separates the bottom 25% of the ordered data from the top 75%, quartile 2, also known as the median or second quartile is the value at which 50% of the data are above and 50% are below, quartile 3 is the value that separates the top 75% of the ordered data from the bottom 25%, minimum is the smallest value in a data set, maximum is the largest value in a data set.

These statistical measures provide important information about the distribution and structure of a data set, which can help in the analysis and interpretation of the data.

Table 3. Results of 50 points taken from electric and magnetic field within the S/E

Data within the S/E		
Data	**Electric field**	**Magnetic field**
Half	1389,18776	1,36405
Median	884,35	1,299
Standard deviation	1325,789867	1,119426703
Quartile 1 al 25%	467,65	0,78825
Quartile 2 al 50%	884,35	1,299
Quartile 3 al 75%	2066	1,51225
Minimum	2,078	0
Maximum	5313	7,387

Table 4. Results of 4 points taken from electric and magnetic field at the S/E boundaries

S/E boundary data		
Data	**Electric field**	**Magnetic fiel**
Half	216,765	1,287
Median	175,7	1,283
Standard deviation	200,1612239	0,050444689
Quartile 1 al 25%	49,195	1,24125
Quartile 2 al 50%	175,7	1,283
Quartile 3 al 75%	425,4	1,33675
Minimum	28,76	1,23
Maximum	486,9	1,352

3.4 Graphical Representation of MLS Method

To visualize the coordinates of the points evaluated at the station, a plot of the scattered points of the **x** and **y** coordinates is made. It is shown in Figure 4.

When creating the scatter plot, it is important to properly configure the axes and scales so that the points are distributed in a clear and understandable way. You can add labels to the axes, a legend if necessary, and other graphical elements that help to better interpret the data.

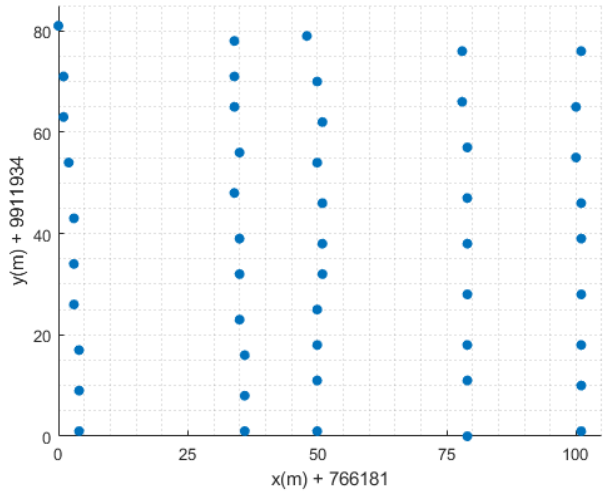

Fig. 4: Coordinates of the measurement points

Each point has an associated electric field and magnetic field value. Because the measurements were taken under difficult field access conditions, the data obtained are not perfectly aligned and do not form a perfectly gridded grid. It is shown in Figure 5.

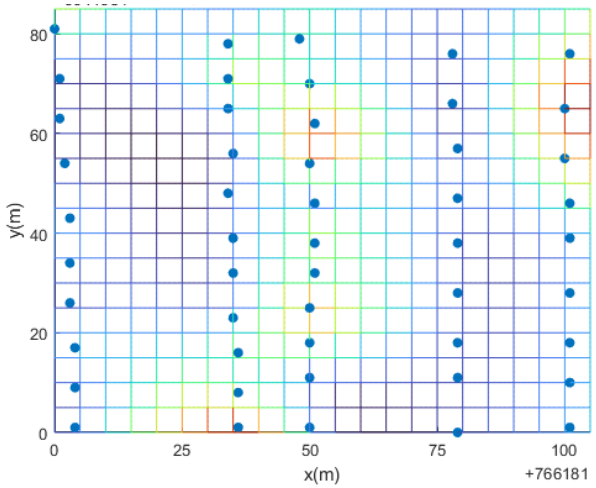

Fig. 5: Electric field measurement adjustment grid

The following Figure 6, Figure 7, and Figure 8 show the mesh and grids adjustment.

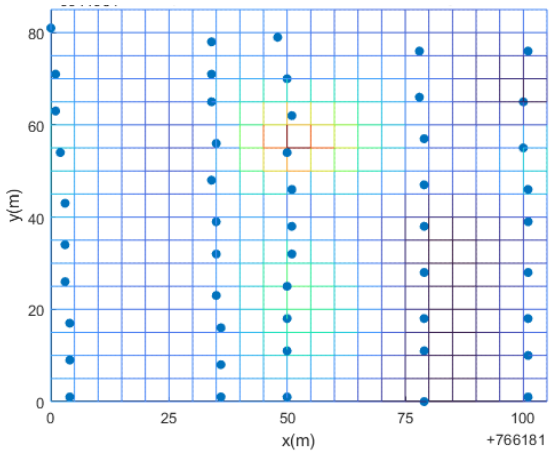

Fig. 6: Magnetic field measurement adjustment grid

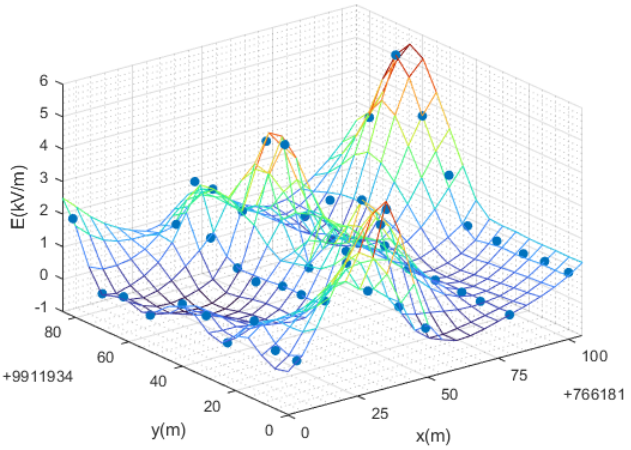

Fig. 7: Adjustment grids for electric field measurements with critical points

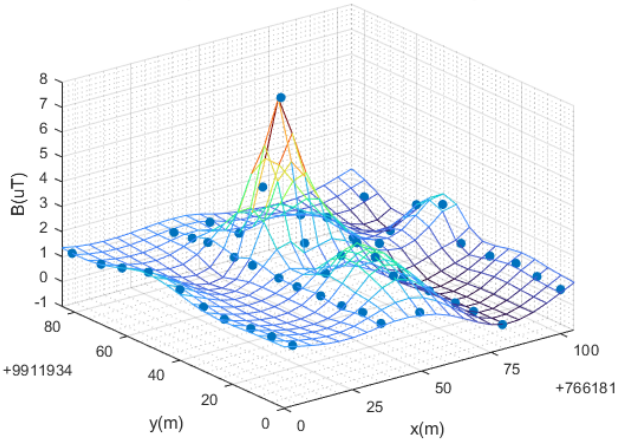

Fig. 8: Adjustment grids for magnetic field measurements with critical points

Therefore, part of the data preprocessing is to generate a perfectly spaced grid by interpolating the collected data, as this shows the most critical points in both CEM, as shown in Figure 7 and Figure 8.

4 Simulation

The result of applying the MLS adjustment is shown below. It can be seen that now the results are displayed for a finer grid, exactly 1m by 1m, previously coarser 5m by 5m.

This gives the appearance of a continuous surface, thus meeting the criteria for the application of MLS for data refinement.

In Figure 9, the electric field and contour lines of a point charge show how an electric charge generates a force in the surrounding space. The direction of the electric field indicates the direction and magnitude of this force, being more intense near the charge. Contour lines, or equipotential lines, are perpendicular to these curves and represent regions where the electric potential is constant. This diagram visualizes the relationship between electric field and potential, facilitating the understanding of fundamental concepts in electromagnetism.

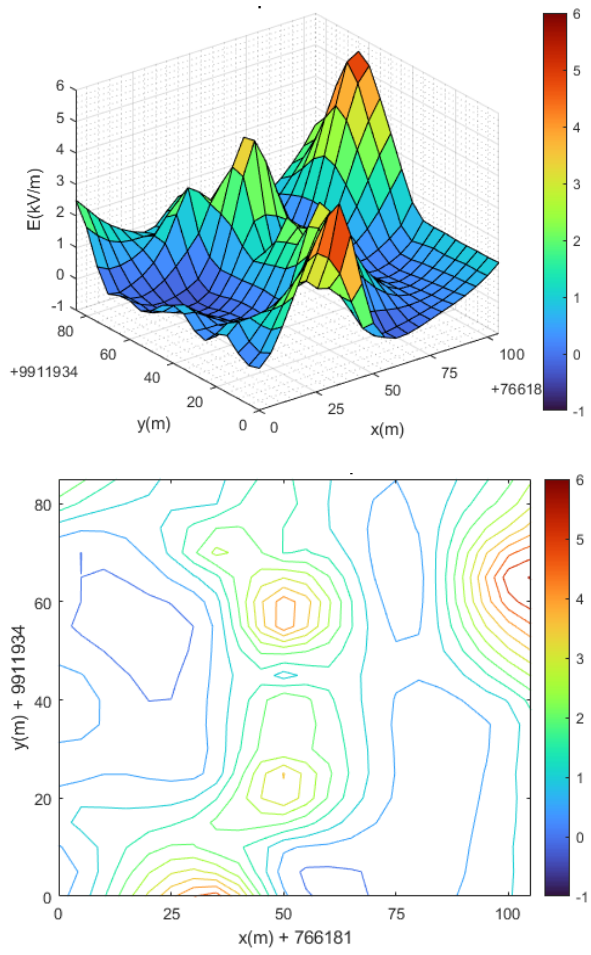

Fig. 9: Original electric field and its respective contour lines

In Figure 10, the electric field and contour lines fitted with MLS provide an accurate and smoothed representation of the field behavior in the presence of multiple charges or complex distributions. MLS allows to fit the experimental electric field data to minimize errors and to obtain a continuous and differentiated model of the field and its equipotentials. This technique is useful for analyzing real systems where the charge distributions are not ideal, improving the accuracy in the prediction and visualization of the electric field and its associated potential.

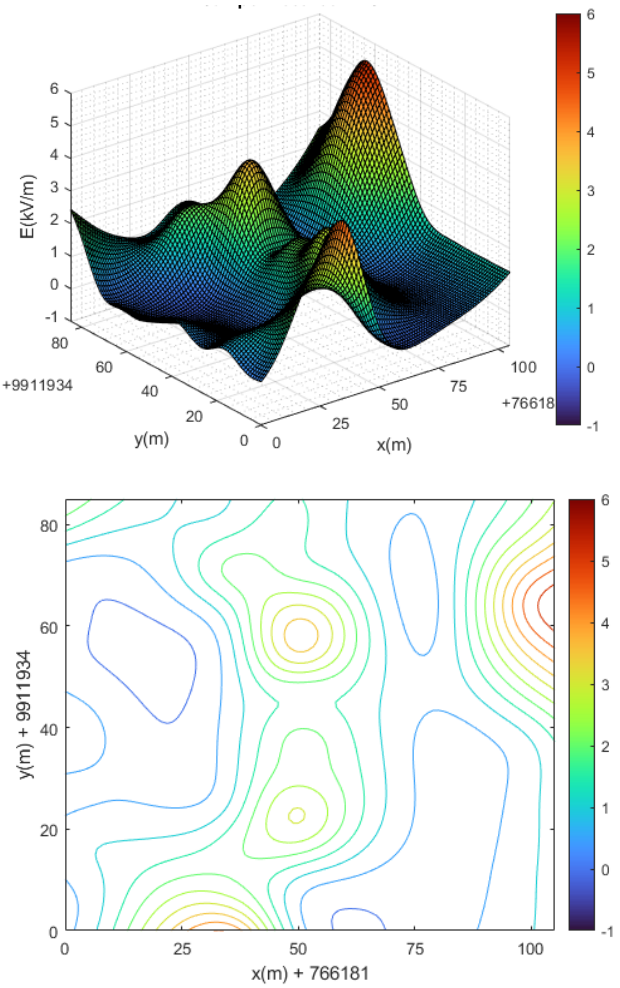

Fig. 10: Electric field and contour lines fitted with MLS

If we distinguish between these two representations, it is clear that the electric field with a point charge and the contour allows us to understand the relationship between the charge dynamics, the electric field strength, and the potential.

In Figure 11, the initial magnetic field generated by an electric current shows a configuration of lines creating closed loops, indicating both the orientation and magnitude of the field. These magnetic field lines show a higher density in the vicinity of the source, suggesting an increase in field strength. Contour lines showing the magnetic potential are perpendicular to the field lines and delineate regions of constant magnetic potential. This representation is crucial

for understanding the interactions between magnetic fields and materials, as well as electric currents in various technological and scientific fields.

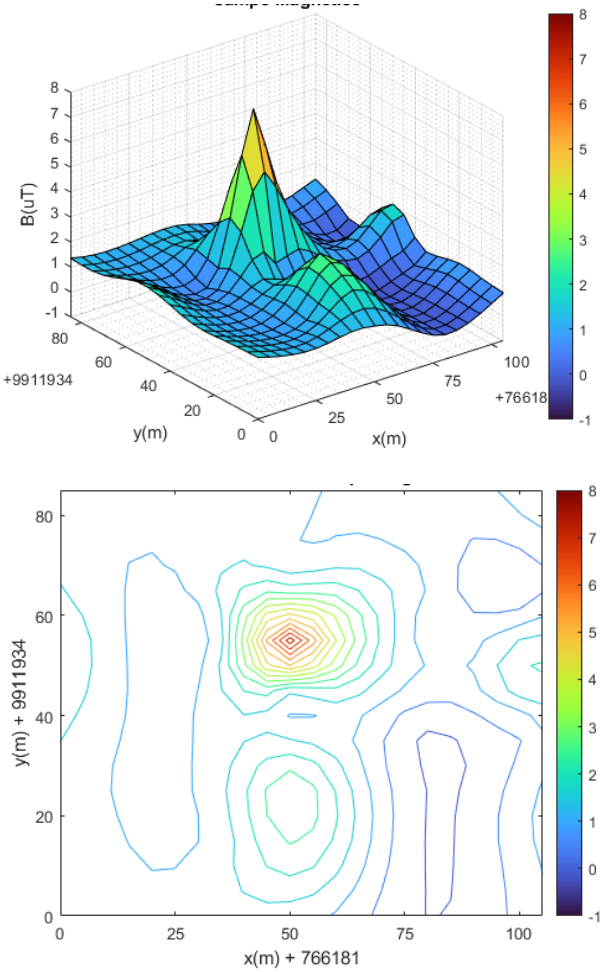

Fig. 11: Original magnetic field and its respective contour lines

In Figure 12, the integration of the magnetic field with contour lines, enhanced by the MLS technique, provides a representation of magnetic phenomena within systems. The MLS methodology allows to synchronize the experimental data of the magnetic field, thus minimizing inaccuracies and obtaining a complete model, even in the midst of irregular current distributions. This methodology is indispensable for accurate analysis in practical applications, thus improving the capability of magnetic behavior in real devices and systems.

The magnetic field and its contour lines associated with the field function generated by a magnet or an electric current. Although they serve to elucidate fundamental principles, they fail to adequately capture the complexities inherent in real systems. In contrast, MLS-enhanced magnetic field and contour lines provide a more accurate and realistic modeling approach, facilitating smoothing of experimental data and addressing complexities to current and material distributions. While the original model is ideal for theoretical illustrations, MLS fitting is essential for detailed practical applications.

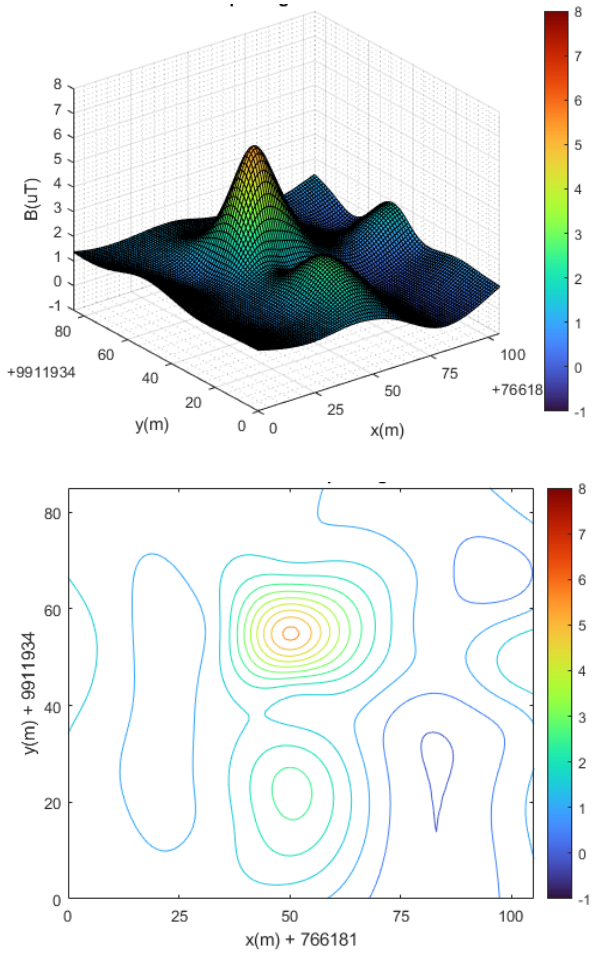

Fig. 12: Magnetic field and contour lines adjusted with MLS

5 Additional Information

5.1 Remarks

The purpose of the measurements was to evaluate the electric and magnetic field generated at the MULALO transmission substation, to which the personnel who work there and the general public are exposed. The monitoring was carried out at 50 points within the facilities and 4 points on the substation boundaries in order to be able to cover all the behavior of the energy sources.

The results obtained inside the substation with respect to the Maximum Exposure Criteria for occupationally exposed personnel do not exceed the reference levels established in current regulations as shown in Table 4, likewise the results obtained at the boundaries of the substation with respect to the Maximum Exposure Criteria for the general public do not exceed the reference limits established in current regulations.

5.2 Location of Measurement Points

The sketch of the location of the measurement points is presented below.

5.2.1 Measurement Points within the Substation

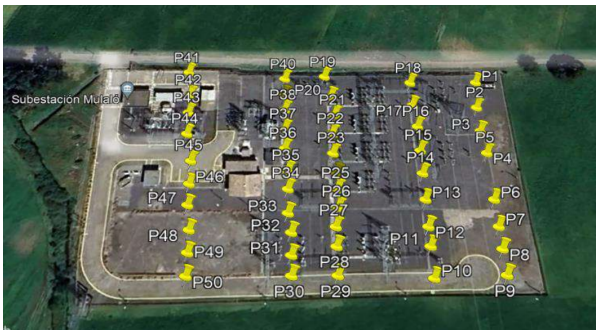

Fig. 13: Measurement points within the S/E

Figure 13 shows a sketch of the 50 measurement points used for the investigation.

The image presents an aerial perspective of the Mulaló Substation, where numerous points of interest are prominently marked with yellow pins and alphanumeric labels. These points, identified with numbers ranging from P1 to P50, are systematically arranged in an organized grid of rows and columns across the substation. The bounded area appears to be segmented into several sections, and it is possible that the numbers assigned to each point refer to equipment, structures, or poles in the facility. The structured design implies that the identified elements adhere to a specific configuration within the substation, characteristic of this type of facility in terms of the systematic arrangement of electrical components, including transformers, transmission lines and other essential apparatus. In addition, it can be observed that certain sections of the substation have a higher concentration of points, which may correspond to areas of increased activity or aggregation of electrical equipment.

5.2.2 Substation Boundary Measurement Points

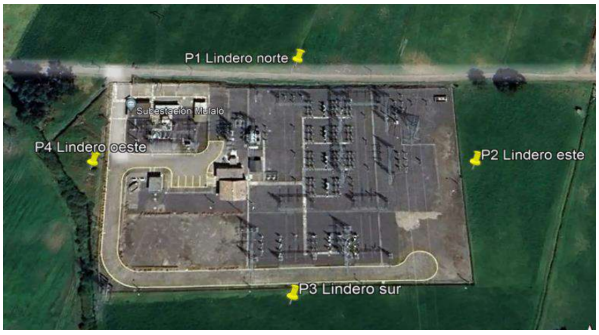

Fig. 14: Measurement points of the S/E boundaries

Figure 14 shows a sketch of the 4 measurement points used for the investigation.

The diagram presents a panoramic view of the Mulaló electrical substation, with perimeter delineations indicated at four designated points.

The reference coordinates indicated in the image (P1, P2, P3 and P4) can serve as critical data points for environmental impact assessments, electromagnetic field monitoring, perimeter security measures or for possible facility expansions. The exact location of these coordinates establishes a framework for systematic inspections and maintenance operations or for the formulation of technical evaluations at the substation.

6 Conclusion

The results acquired within the substation concerning the Maximum Non-Ionizing Radiation Exposure Criteria for personnel exposed in occupational settings indicate conformity with the reference levels set forth in the prevailing regulations. These outcomes signify that the exposure levels are within acceptable limits and do not surpass the thresholds established to safeguard the health and safety of workers who may encounter non-ionizing radiation in their professional environment. Moreover, the analysis guarantees a confidence level of approximately 95%, considering the measurement uncertainty associated with the data. This elevated confidence level underscores the dependability of the results and reinforces the conclusion that the exposure levels remain significantly below the maximum permissible limits, thereby mitigating potential health risks to personnel operating in such environments. This compliance with the established criteria ensures the execution of safety measures consistent with regulatory standards, thereby enhancing the overall safety and well-being of the workforce.

The maximum measured value for the electric field is 5.313 kV/m, while the maximum value for the electric field adjusted with MLS is 5.335 kV/m. If we take the field measurement value as the accepted value, we have that the variation between the adjusted value and the accepted value is 0.41%. Similarly, the maximum value measured for the magnetic field is 7.387 uT, while the adjusted value is 5.625 uT; being the variation of 23.84%.

The refined values derived from the MLS methodology for the electric field demonstrate an average deviation of approximately 0.53% when juxtaposed with the values obtained through direct on-site measurements. This slight deviation signifies a substantial concordance between the adjusted model values and the empirical field measurements, implying that the MLS adjustments yield a dependable representation of the electric field. Conversely, the adjusted values for the magnetic

field reveal a more significant average deviation of around 5.85% in relation to the values acquired on-site. While this deviation is somewhat greater than that noted for the electric field, it remains within permissible thresholds, suggesting that the adjusted magnetic field values still offer a reasonably precise estimation of the actual conditions. This discrepancy may be ascribed to a range of factors, including measurement uncertainties, environmental impacts, or the intrinsic complexities associated with modeling magnetic field dynamics in fluctuating substation settings.

Based on the percentage of fit between the values taken in the field and those fitted by the MLS method, it can be said that the smoothing for the electric field was not so significant, while it was significant for the magnetic field. This is quite common, since the electric field values present variations in the whole region; while in the magnetic field it is almost flat with a single concentrated peak. The MLS setting ”smooths” and ”flattens” the surfaces, with the magnetic field being more affected than the electric field.

Acknowledgment:

The students, Beltrán Romina and Chamorro Emily, are grateful for the guidance and support provided by professors Quinatoa Carlos and Toaza Jimmy, for their guidance throughout the research, whose support has been essential to ensure a thorough and complete work.

Statement:

During the preparation of this article, the authors used Grammarly for linguistic proofreading. After using this site, the authors reviewed and edited the content as necessary and assume full responsibility for the content of the publication.

References:

[1] E. Salinas, “Passive and active shielding of power-frequency magnetic fields from secondary substation components,” vol. 2, pp. 855–860, 2000.

[2] T. Keikko, R. Pääkkönen, S. Kännälä, R. Seesvuori, and S. Valkealahti, “Magnetic field risk evaluation of workers in indoor distribution substations,” pp. 1–4, 2009.

[3] M. Misakian, “Extremely low frequency electric and magnetic field measurement methods,” pp. 451–457, Springer, Boston, MA, 1998.

[4] O. E. Okoye, B. Atisi, M. Idonje, and E. O. Agbalagba, “Evaluating the effect of electromagnetic field from electrical distribution substations in aguata, nigeria,” *International journal of research and innovation in applied science*, vol. IX, no. VI, pp. 414–424, 2023.

[5] M. A. Zazouli, M. Mohammadyan, S. N. Mousavinasab, M. M. Darabi, and A. S. Safari, “Magnetic flux emission from extremely low frequency electromagnetic fields around high voltage power transmission lines,” *Journal of Mazandaran University of Medical Sciences*, vol. 28, no. 169, pp. 140–150, 2019.

[6] S. Özden, B. S. Aral, A. C. Kurşun, and N. Seyhan, “Measurement and risk assessment of extremely low frequency magnetic fields around transformers in a working place,” vol. 13, no. 2, pp. 857–867, 2020.

[7] P. Nassiri, M. R. Monazzam, S. A. Hosseyni, K. Azam, and P. J. Shalkouhi, “Extremely low-frequency electromagnetic field due to power substations in urban environment,” *Environmental Engineering and Management Journal*, vol. 17, no. 8, pp. 1825–1830, 2018.

[8] K. Friedl, A. Abart, R. Schürhuber, and E. Schmautzer, “Standardised evaluation of the electric field for meeting safety aspects for workers according to directive 2013/35/eu and vemf,” *Elektrotechnik Und Informationstechnik*, vol. 136, no. 8, pp. 352–360, 2019.

[9] Q.-z. Qin, Y. Chen, T.-t. Fu, L. Ding, L.-l. Han, and J.-c. Li, “The monitoring results of electromagnetic radiation of 110-kV high-voltage lines in one urban location in Chongqing P.R. China,” *Environmental Monitoring and Assessment*, vol. 184, no. 3, pp. 1533–1540, 2012.

[10] H. Liu, G. Chen, Y. Pan, Z. Chen, W. Jin, C. Sun, C. Chen, X. Dong, K. Chen, Z. Xu, S. Zhang, and Y. Yu, “Occupational Electromagnetic Field Exposures Associated with Sleep Quality: A Cross-Sectional Study,” *PLOS ONE*, vol. 9, no. 10, pp. 1–8, 2014.

[11] R. Stam and S. Yamaguchi-Sekino, “Occupational exposure to electromagnetic fields from medical sources,” *Industrial Health*, vol. 56, no. 2, pp. 96–105, 2018.

[12] R. Gallego-Martínez, F. J. Muñoz-Gutiérrez, and A. Rodríguez-Gómez, “Trajectory optimization for exposure to minimal electromagnetic pollution using genetic

algorithms approach: A case study," *Expert Systems with Applications*, vol. 207, p. 118088, 2022.

[13] S. Esmailzadeh, M. A. Delavar, A. Aleyassin, S. A. Gholamian, and A. Ahmadi, "Exposure to Electromagnetic Fields of High Voltage Overhead Power Lines and Female Infertility.," *The international journal of occupational and environmental medicine*, vol. 10, pp. 11–16, jan 2019.

[14] A. Ayuso-Álvarez, J. García-Pérez, J.-M. Triviño-Juárez, U. Larrinaga-Torrontegui, M. González-Sánchez, R. Ramis, E. Boldo, G. López-Abente, I. Galán, and P. Fernández-Navarro, "Association between proximity to industrial chemical installations and cancer mortality in Spain," *Environmental Pollution*, vol. 260, p. 113869, 2020.

[15] X. Zhao, J. Wang, Y. Gao, and T. Chen, "The fuzzy comprehensive evaluation on occupational health hazards of electric field in substation," *AIP Conference Proceedings*, vol. 1839, 2017.

[16] J. C. Muñoz-Mateos, A. Gil De Paz, S. Boissier, J. Zamorano, D. A. Dale, P. G. Pérez-González, J. Gallego, B. F. Madore, G. Bendo, M. D. Thornley, B. T. Draine, A. Boselli, V. Buat, D. Calzetti, J. Moustakas, and R. C. Kennicutt, "Radial distribution of stars, gas, and dust in sings galaxies. ii. derived dust properties," *Astrophysical Journal*, vol. 701, no. 2, pp. 1965–1991, 2009.

[17] A. M. García, "Pesticide exposure and women's health.," *American journal of industrial medicine*, vol. 44, pp. 584–594, dec 2003.

[18] J. A. Heredia-Rojas, A. O. la Fuente, R. Gomez-Flores, O. Heredia-Rodríguez, L. E. Rodríguez-Flores, M. Beltcheva, and M. E. Castañeda-Garza, "In Vivo Cytotoxicity Induced by 60 Hz Electromagnetic Fields under a High-Voltage Substation Environment," *Sustainability*, vol. 10, no. 8, 2018.

[19] E. Lumnitzer, E. L. Jurgovska, M. Andrejiova, and R. Kralikova, "Application of Metal Shielding Materials to Protect Buildings Occupants from Exposure to the Electromagnetic Fields," *Materials*, vol. 16, no. 15, 2023.

[20] TULSMA, "Unified Text of Secondary Legislation of the Ministry of the Environment, TULSMA," *Registro Oficial Edición Especial 2 de 31-mar.-2003*, no. 3399, p. 407, 2017.

[21] "IEEE Standard Procedures for Measurement of Power Frequency Electric and Magnetic Fields from AC Power Lines," *IEEE Std 644-2019 (Revision of IEEE Std 644-2008)*, pp. 1–40, 2020.

[22] H. Zhang, C. Guo, X. Su, and C. Zhu, "Measurement data fitting based on moving least squares method," *Mathematical Problems in Engineering*, vol. 2015, 2015.

Contribution of Individual Authors to the Creation of a Scientific Article (Ghostwriting Policy)

Beltran Romina and Chamorro Emily are responsible for the original writing of the article based on adequate research, reinforcing the validity of the findings through data collection and corresponding analysis through simulation.

Carlos Quinatoa and Jimmy Toaza played the role of teacher guides, dedicated to providing guidance and supervision for the research and analysis of the appropriate results, also providing theoretical and technical advice in order to ensure a good inquiry, as their experience and knowledge are crucial to ensure a rigorous and ethical work.

Sources of Funding for Research Presented in a Scientific Article or Scientific Article Itself

No funding was received for conducting this study.

Conflicts of Interest

The authors state that they have no financial interests or personal relationships that could affect the work done in this study.